Citation: Cell Death and Disease (2011) 2, e203; doi:10.1038/cddis.2011.87

www.nature.com/cddis

Targeting neonatal ischemic brain injury with a pentapeptide-based irreversible caspase inhibitor

D Chauvier[1,2], S Renolleau[3,4,5], S Holifanjaniaina[6,7], S Ankri[1,2], M Bezault[1,2], L Schwendimann[6,7], C Rousset[8,9], R Casimir[1,2,10], J Hoebeke[10], M Smirnova[1,2], G Debret[11,12], A-P Trichet[2], Y Carlsson[9,13], X Wang[9], E Bernard[2], M Hébert[2], J-M Rauzier[14,15], S Matecki[16,17], A Lacampagne[15,17], P Rustin[6,7], J Mariani[3,4,18], H Hagberg[8,9,13], P Gressens[6,7,8], C Charriaut-Marlangue[3,4] and E Jacotot*[,1,2,6,7,8]

Brain protection of the newborn remains a challenging priority and represents a totally unmet medical need. Pharmacological inhibition of caspases appears as a promising strategy for neuroprotection. In a translational perspective, we have developed a pentapeptide-based group II caspase inhibitor, TRP601/ORPHA133563, which reaches the brain, and inhibits caspases activation, mitochondrial release of cytochrome *c*, and apoptosis *in vivo*. Single administration of TRP601 protects newborn rodent brain against excitotoxicity, hypoxia–ischemia, and perinatal arterial stroke with a 6-h therapeutic time window, and has no adverse effects on physiological parameters. Safety pharmacology investigations, and toxicology studies in rodent and canine neonates, suggest that TRP601 is a lead compound for further drug development to treat ischemic brain damage in human newborns.

Cell Death and Disease (2011) **2,** e203; doi:10.1038/cddis.2011.87; published online 1 September 2011
Subject Category: Neuroscience

Worldwide estimations indicate more than 2 million non-infectious neonatal deaths per year.[1] Neonatal ischemic brain injuries, such as stroke (focal cerebral ischemia involving middle cerebral artery occlusion (MCAO)) or hypoxia–ischemia (HI) (involving systemic asphyxia), are major and untreated causes of newborn morbidity and mortality.[2,3] Of the infants who survive the first few hours after intrapartum-related neonatal deaths (previously called 'birth asphyxia'), as many as an annual 1 million may develop cerebral palsy, learning difficulties or other disabilities.[4] Recent clinical trials show that therapeutic intervention by brain cooling beginning up to 6 h after perinatal asphyxia reduces cerebral injury and improves outcomes in term infants.[5] Although these studies provide proof of concept that in this context cell death is both delayed and preventable, the protection is limited and there is still no treatment available for perinatal stroke or brain injury occurring in preterm infants.[6]

Ischemic brain injury in the developing brain involves several factors such as excitotoxicity, oxidative stress, and inflammation, which accelerate cell death through either apoptosis or necrosis, depending on the region of the brain affected and on the severity of the insult.[7,8] Accumulating data suggest that apoptotic mechanisms have a more prominent role in the evolution of ischemic brain injury in neonatal rodents[9–11] and humans[12] than in adult brain ischemia,[13,14] and that apoptosis involves the mitochondrial release of cytochrome *c*[11] and apoptosis-inducing factor (AIF),[11,15,16] which activate caspase-dependent[10,16] and -independent execution pathways,[13,16] respectively.

Caspases are a class of cysteine endoproteases that have strict specificity for an aspartic residue at the S1 subsite.[17,18] Some caspases are important mediators of inflammation and others are involved in the apoptosis of mammalian cells, where they participate in signaling and effector pathways.[19] On the basis of the optimal four-amino-acid sequence to the left of the cleavage site, caspases may be classified into three groups: group I contains caspase-1, -4, and -5 (optimal tetrapeptide: WEHD), group II contains caspase-2 (Casp2), -3 (Casp3), and -7 (Casp7) (optimal tetrapeptide: D[E/A]XD), and group III contains caspase-6, -8 (Casp8), -9 (Casp9), and -10 (optimal tetrapeptide: [V/L]EXD).[20–22]

[1]Theraptosis Research Laboratory, Theraptosis SA, Pasteur BioTop, Institut Pasteur, Paris 75015, France; [2]Theraptosis R&D Laboratories, Theraptosis SA, Biocitech Technology Park, Romainville 93230, France; [3]CNRS, UMR 7102 NPA, Paris 75005, France; [4]Pierre and Marie Curie University Paris 6, UMR 7102 NPA, Paris 75005, France; [5]Service de Réanimation Néonatale et Pédiatrique, Hôpital Armand Trousseau - APHP, Paris 75012, France; [6]Inserm, U676, Paris 75019, France; [7]Université Paris Diderot, UMR 676, Paris 75019, France; [8]Centre for the Developing Brain, Institute of Reproductive and Developmental Biology, Imperial College London, Hammersmith Hospital, London W12 0NN, UK; [9]Department of Physiology, Perinatal Center, Sahlgrenska Academy, Göteborg University, Gothenburg 40530, Sweden; [10]CNRS UPR 9021, Institut de Biologie Moléculaire et Cellulaire, Strasbourg 67084, France; [11]Laboratoire de Physique Théorique de la Matière Condensée, CNRS UMR 7600, Paris 75005, France; [12]Pierre and Marie Curie University Paris 6 UMR 7600 LPTMC, Paris 75005, France; [13]Department of Obstetrics and Gynaecology, Sahlgrenska University Hospital, Gothenburg 41345, Sweden; [14]CHU de Nîmes, Nîmes 30000, France; [15]Inserm U1046, Montpellier 34925, France; [16]CHU de Montpellier, Montpellier 34925, France; [17]Université Montpellier 1 et 2, Montpellier 34925, France and [18]Hôpital Charles Foix, UEF, Ivry-sur-Seine 94205, France
*Corresponding author: E Jacotot, Inserm, U676, Hôpital Robert Debré, 48 Bd Sérurier, Paris 75019, France. Tel: +33 1 4003 1932; Fax: +44 20 7594 2154;
E-mail: etienne.jacotot@inserm.fr or e.jacotot@imperial.ac.uk

Keywords: caspase inhibitor; perinatal brain damage; ischemia; neuroprotection

Abbreviations: AIF, apoptosis-inducing factor; Casp2, caspase-2; Casp3, caspase-3; Casp8, caspase-8; Casp9, caspase-9; Casp7, caspase-7; Δ2Me-TRP601, TRP601 devoid of methyl ester groups on Asp lateral chains; ECG, electrocardiogram; HI, hypoxia–ischemia; i.p., intraperitoneal; i.v., intravenous; MCAO, middle cerebral artery occlusion; Q-VD-Oph, quinoline-Val-Asp-CH2-OPh; TUNEL, terminal deoxynucleotidyl transferase dUTP nick-end labeling; SD, serum deprivation; z-VAD-fmk, *N*-benzyloxycarbonyl-Val-Ala-Asp(Ome)-fluoromethylketone

Received 20.7.11; accepted 21.7.11; Edited by D Bano

Both pancaspase inhibition and Casp3-selective inhibition have been reported to be neuroprotective in various rodent models of neonatal brain injury,[13,23,24] opening the possibility for pharmacological intervention.[6] However, lack of protection with caspase inhibitors was also reported,[25,26] possibly reflecting differences between experimental models or settings (e.g., the age of animals[26]), specific *in vivo* properties of the used inhibitors (e.g., brain penetration[27]), and/or a shift to caspase-independent cell death pathways (e.g., AIF, autophagic death, necroptosis).

The role of individual caspases in the developing brain is not fully understood. Genetic analysis using constitutive deficiency revealed that Casp3 and Casp9 execute programmed (physiological) cell death in the central nervous system,[28,29] whereas Casp2 does not.[30] Aggravation of HI-induced lesions was reported in Casp3-null mice.[31] In contrast, genetic inhibition of Casp2 is neuroprotective in newborn mice exposed to HI or excitotoxic challenges.[32]

In a translational attempt to generate an efficient and safe Casp2/group-II caspase inhibitor, we have developed a potent pentapeptide-based irreversible caspase inhibitor. We report here the preclinical evaluation of this compound and present data supporting a potent neuroprotective role against perinatal ischemic brain damage in a variety of *in vivo* models, potentially opening an avenue for treatment.

Results

Design of a caspase inhibitor adapted for neuroprotection in neonates. We previously showed that the pancaspase inhibitor quinolyl-carbonyl-Val-Asp-difluorophenoxymethylketone (Q-VD-OPh) has enhanced *in vitro* and *in vivo* pharmacological properties,[33] together with potent neuroprotective effects in neonatal brain injury experimental models.[10,16,34] We reasoned that an *in vivo* efficient group II-selective caspase inhibitor might combine an amino-terminal quinolyl-carbonyl and a C-terminal fluorophenoxymethyl ketone warhead ($CH_2OC_6H_3$-F_2) with the Casp2-preferred pentapeptide backbone VDVAD,[20,33,35,36] a sequence that is also efficient as a substrate for Casp3,[37] but is a weaker substrate for group-I and -III caspases (data not shown and McStay *et al.*[37]). Using the reported Casp2 crystallographic data,[38] we modeled pentapeptide structures within the Casp2 active site (Figure 1a and Supplementary Figure S1), and chose to add methyl ester group to the lateral chain of each Asp residues to enhance lipophilicity (a well-known approach to promote blood–brain barrier penetration) and delay degradation by proteases *in vivo*. The resulting substituted pentapeptide quinolin-2-carbonyl-VD(OMe)VAD(OMe)-CH_2-O(2,6F_2)Ph (referred thereafter as TRP601) was selected (Figure 1b). TRP601 is an irreversible caspase inhibitor that, similar to other VDVAD-based inhibitors,[20,21,37] is a potent inhibitor of group II caspases. Indeed, *in vitro* kinetic analysis showed that TRP601 potently inhibits Casp3 ($IC_{50/Casp3/TRP601} = 47.3 \pm 11.2$ nM; $k_3/K_i = 36\,025$/M/s; $n = 3$) and also inhibits recombinant Casp2 ($IC_{50/Casp2/TRP601} = 479.8 \pm 79.3$ nM; $k_3/K_i = 1243$/M/s; $n = 3$) (Figures 1c and d). According to its irreversible nature, TRP601 showed a fourfold IC_{50} reduction if preincubated 45 min with Casp2 before substrate addition ($IC_{50/rCasp2/TRP601/45\,min} = 127 \pm 25$ nM; $n = 3$**)**.

As expected, TRP601 had no substantial activity outside the caspase family, as found in a binding screen of 110 different receptors, transporters and ion channels, and 56 enzyme activity assays, including calpains, various cathepsins (B, H, G, L), granzyme B, and several glutamatergic sites such as *N*-methyl-D-aspartatic acid and α-amino-3-hydroxy-5-methyl-4-isoxazole propionic acid (Table 1). When used in cell culture assays like serum-deprived primary embryonic cortical neurons,[39] TRP601 prevented caspase activation and cell death (Figure 1e). Following intravenous (i.v.) administration in adult rats, TRP601 quickly entered the brain (Figure 1f; $T_{max} = 25$ min in the brain; $C_{max} = 120$ ng/ml in the brain, 1 mg/kg, i.v. bolus dose). Interestingly, an active metabolite Δ2Me-TRP601 (TRP601 devoid of methyl ester

Figure 1 Design and pharmacological evaluation of TRP601. (**a)** Substrate binding region of caspase-2 (Casp2) in complex with TRP601. The quinolin-2-carbonyl-Val-Asp(OMe)-Val-Ala-Asp(OMe)-CH_2- moiety is shown in sticks representation with the atoms represented as follows: gray = carbon; white = hydrogen; blue = nitrogen; and red = oxygen. The S–C covalent bond between the Cys-155 residue and the C terminus CH_2 of TRP601 is represented in yellow. The electric interactions (hydrogen bonds and salts bridges) are represented by the dashed, green lines. The enzyme residues that interact with the inhibitor are shown by the wireframe representation. Right panel: the table shows the minimal energy (kcal/mol, E_{min}) of the Casp2–TRP601 complex resulting from electric or Coulombic component (E_c) together with repulsion–attraction component (E_{vw}). The interaction energy of the Casp2–TRP601 complex is −147.28 kcal/mol. Owing to the C–S covalent bond, the Asp residue in P1 contributes to about 30% of the interaction energy. The Asp in P4 and the Val in P5 have important non-covalent contributions to stabilization of the complex, 21% and 17%, respectively. Each of the other two residues (Ala in P2 and Val in P3) contributes to about 12% of the interaction energy. (**b**) Structure of TRP601. (**c**) Representative dose–response curve of human recombinant Casp2 and Casp3 inhibition by TRP601. Initial velocities were determined from standard colorimetric microplate assays. (**d**) Kinetic *off rate (k_3/K_i)* parameters of irreversible caspase inhibitors on Casp2 and Casp3. (**e**) TRP601 inhibits neuronal caspase activities and prevents serum deprivation (SD)-induced cell death. High-density E14 cortical neuron cultures were subjected to 24 h SD in the presence or absence of 50 μM TRP601. Histograms indicate the means (± S.D.) of 15 independent experiments. (**f**) Representative pharmacokinetic of TRP601 after intravenous (i.v.) administration in adult rats, through liquid chromatography-mass spectrometry (LC-MS/MS) detection in the plasma and brain homogenates. Note that following intraperitoneal (i.p.) administration of the same dose, TRP601 was detected in the brain at 0.25 h (brain $C_{max} = 25$ ng/ml) and the C_{max} (20 ng/ml) was obtained in the plasma according to a plateau between 0.5 and 2 h. (**g–j**) TRP601 reduces excitotoxic lesions in neonates. The 5-day-old mice were subjected to intracerebral ibotenate injection and killed at different time points (**g** = 5 days; **h** and **i** = 24 h; **j** = 8 h) following the excitotoxic challenge to determine the impact of TRP601, TRP801, and TRP901 (1 mg/kg; i.p.) on lesion severity (**g**), microgliosis (**h**), astrogliosis (**i**), and group II caspases activity (**j**). Histograms show mean lesion volume (**g**; ■, vehicle, $n = 16$; TRP601, $n = 16$; TRP801, $n = 7$; TRP901, $n = 8$), cell density (**h** and **i**; $n = 10$ per group), or VDVADase activity (**j**; $n = 5$ per group) ± S.E.M. Asterisks indicate differences from control (■) (*$P < 0.05$, **$P < 0.01$, ***$P < 0.001$ in Kruskal–Wallis *post hoc* Dunn's for **g**, Mann–Whitney for **h–j**). (**k**) TRP601 does not enhance protection conferred by short interfering RNA (siRNA)-mediated genetic inhibition of Casp2. The 5-day-old mice were subjected to intracerebral injection (as in **c**) of either an siRNA against Casp2 (si2-a) or a control siRNA (si2Co), as indicated. After 24 h, ibotenate was administered (intracerebroventrally (i.c.v.)), followed immediately by vehicle (□, $n = 20$; ■, $n = 20$) or TRP601 (■; $n = 24$) administration (i.p.). See Supplementary Table 1 for exact values and detailed statistical analysis

a

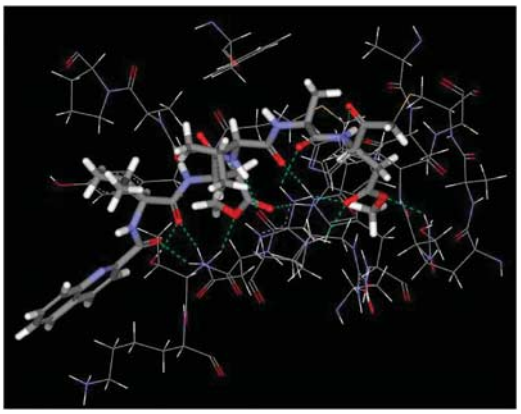

Fragment	E min (Kcal/mol)	E vw (Kcal/mol)	E c (Kcal/mol)
P1 Asp and C-S covalent bond	-43.86	-17.78	-26.08
P2 Ala	-17.31	-6.40	-10.91
P3 Vla	-17.16	-7.95	-9.21
P4 Asp	-30.82	-11.74	-19.09
P5 Val	-25.28	-8.52	-16.76
quinolin-2-carbonyl	-12.84	-6.73	-6.11
Sum	**-147.28**	**-59.11**	**-88.17**

b

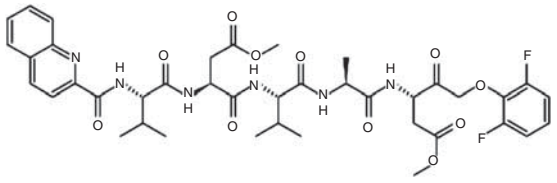

c

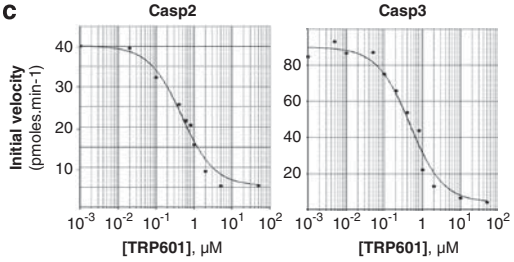

d

	TRP601		Δ2Me-TRP601	
	IC_{50} (nM)	k_3/K_i ($M^{-1}s^{-1}$)	IC_{50} (nM)	k_3/K_i ($M^{-1}s^{-1}$)
Casp2	479.8 ± 79.3	1 243	7.4 ± 3.1	182 801
Casp3	47.3 ± 11.2	36 025	0.42 ± 0.16	34 782 163

e

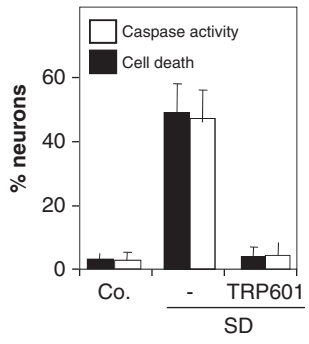

f

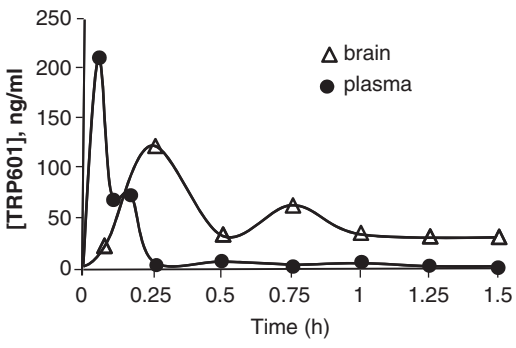

g

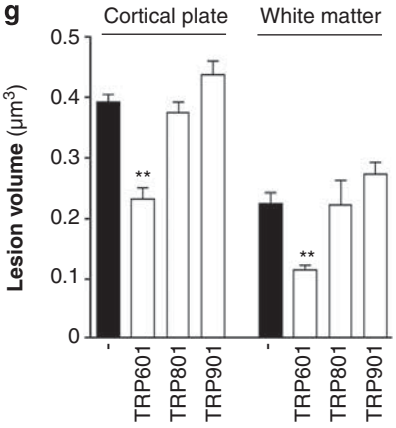

h

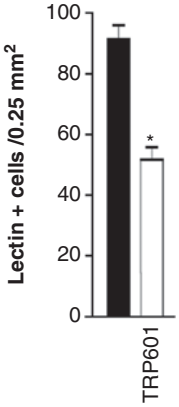

i

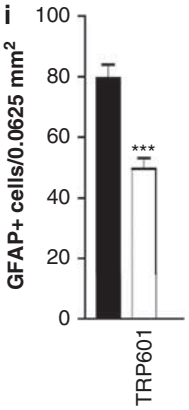

j

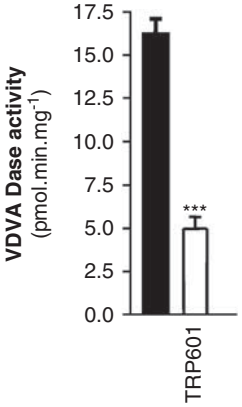

k

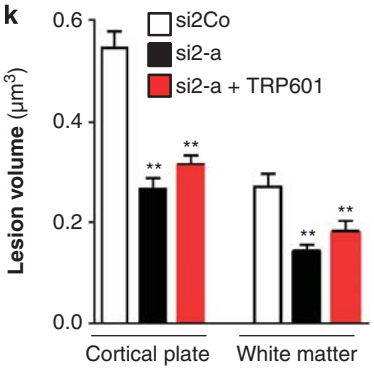

groups on Asp lateral chains) was progressively generated in the blood. We have re-synthesized this metabolite and found that it strongly inhibits Casp3 ($IC_{50/Casp3/\Delta 2Me\text{-}TRP601}$ against recombinant Casp3 (rCasp3) = 0.42 ± 0.16 nM; k_3/K_i = 34 782 163/M/s) and Casp2 ($IC_{50/Casp2/\Delta 2Me\text{-}TRP601}$ against rCasp2 = 7.4 ± 3.1 nM; k_3/K_i = 182 801/M/s; $n = 3$) *in vitro*.

Table 1 Comprehensive *in vitro* pharmacology profile of TRP601

Non-peptide receptors	Peptide receptors	Nuclear receptors
Adenosine	Angiotensin-II	Glucocorticoid
Adrenergic	Bombesin	Estrogen alpha
Cannabinoid	Calcitonin gene-related peptide	Androgen
Dopamine	Chemokine	
GABA	Cholecystokinin	*Ion channels*
Glutamate	Complement 5a	Ca^{2+} channels
Glycine	Endothelin	K^+ channels
Histamine	Galanin	Na^+ channel
Imidazole	Glucagon	
Leukotriene	Growth hormone secretagogue	*Enzymes*
Melatonin	Melanin-concentrating hormone	Kinases
Muscarinic	Motilin	Phosphatases
Nicotinic	Neurokinin	Serine proteases
Purinergic	Neuropeptide Y	Cysteine proteases
Serotonin	Neurotensin	Aspartate proteases
Sigma	Opioid and opioid-like	Arachidonic acid metabolism
	Somatostatin	Prostaglandin metabolism
Amine transporters	Thyroid hormone	Monoamine synthesis and metabolism
Choline	Urotensin-II	Neurotransmitter synthesis and metab.
Dopamine	Vasoactive intestinal peptide	Nitric oxide synthesis
GABA	Rolipram	Second messenger systems
Norepinephrine	Vasopressin	ATPases
Seretonin		Lipid synthesis
		Metalloproteases
		Miscellaneous enzymes

TRP601 (10 μM) did not significantly modify the activity of 56 enzymes and did not impair or increase the binding of specific ligands to their receptors (110 receptors, channels, or transporters tested). Synthetic list of enzymes, peptide and non-peptide receptors, nuclear receptors, ion channels, or amine transporters, challenged with TRP601 (see details in Supplementary Table S3)

Figure 2 TRP601 has neuroprotective effects in a perinatal stroke model. The 7-day-old rats underwent electrocoagulation of the left middle cerebral artery and transient homolateral common carotid artery occlusion for 50 min, followed by 48 h of recovery. (**a**) Pre-treatment with TRP601 confers strong cerebroprotection. Vehicle (■; $n = 15$), 100 μg TRP601 (□; $n = 24$) or 100 μg TRP901 (■; $n = 9$) was injected intraperitoneally (i.p.) before ischemia. Histograms represent mean ± S.E.M. Kruskal–Wallis ($P = 0.0004$), *post hoc* Dunn's ($P < 0.001$ for TRP601 *versus* vehicle). (**b**) Dose–response of TRP601 administered 1 h after MCAO onset ($n = 103$, $P < 0.002$ Kruskal–Wallis). Histograms represent mean ± S.E.M. Asterisks indicate the level of significance in Dunn's *post hoc*. (**c**) Representative cresyl violet-stained coronal sections from vehicle-treated and TRP601-treated (1 mg/kg i.p.; 1 h post-ischemia) animals at 48 h post-reperfusion at the level of dorsal hippocampus and anterior commissure. Dotted lines indicate infarct area. Scale bar = 500 μm. (**d**) Time window for treatment with TRP601 ($n = 274$, $P < 0.0001$ Kruskal–Wallis). Individual percentage infarct volumes at 48 h post-ischemia are shown in vehicle- ($n = 43$) or TRP601-treated rats (1 mg/kg; i.p.) at 1 h ($n = 51$, ***), 2 h ($n = 45$, ***), 3 h ($n = 40$, ***), 4 h ($n = 48$, *), and 6 h ($n = 47$, *) post-occlusion (asterisks indicate the level of significance in Dunn's *post hoc*). Temperature and body weight were systematically monitored in ischemic animals (treated or not with TRP601) and were found unchanged during ischemia, at reperfusion, and up to 48 h post-ischemia. (**e** and **f**) TRP601 effects after intravenous injection. TRP601 was administered intrajugularly 1 h after the ischemic onset ($n = 15$). (**e**) Representative micrographs of entire pup brains at 48 h post-stroke. Arrows indicate electrocoagulation points. Upper micrograph shows representative lesion at 48 h with visible ischemic territory. Lower micrograph is representative for low lesional score found in 33% of animals injected with 0.1 mg/kg TRP601. (**f**) Raustro-caudal profiles (coronal sections of ipsilateral hemisphere) after intravenous (i.v.) administration of TRP601 (1 h after ischemia) at 0.1 mg/kg ($n = 15$) or 1 mg/kg ($n = 16$). (**g** and **h**) TRP601 has long-term protective effects. Vehicle or 0.1 mg/kg TRP601 was i.p. injected 1 h after the ischemic onset. After 21 days of recovery, animals were killed. (**g)** Cresyl violet-stained coronal sections showing brain injury in a representative animal for each treatment (upper: bregma 0.7; lower: −3.3 mm). Note that TRP601 reduces the cortical cavity and tissue loss in external and internal capsule (ec, ic), caudate putamen (CPu), and amygdaloid nucleus (bregma −3.6, −4 mm; data not shown). (**h**) Quantification of the cavity volume (% cavitation) and hemispheric tissue loss (100−% ipsi/contra) in the presence ($n = 12$) or absence ($n = 6$) of TRP601. Data are mean ± S.E.M. (bars) values. $^*P = 0.0017$; $^{\#}P = 0.0192$ (Mann–Whitney). (**i** and **j**) *In vivo* and *ex vivo* cell death, at 48 h post-stroke, in the ipsilateral cortex of vehicle- and TRP601-treated ischemic animals. Propidium iodide was injected intrajugularly (10 mg/kg) into rat pups before ischemia and coronal sections were analyzed by fluorescence microscopy (**i**, representative micrograph; **j**, left histograms). Alternatively, coronal sections were subjected to *in situ* 3′-OH end DNA labeling (terminal deoxynucleotidyl transferase dUTP nick-end labeling , TUNEL), counterstained with Hoechst 33342, and analyzed by fluorescence microscopy (**j**). Data are mean ± S.E.M. (bars) values ($n = 5$). $^{**}P = 0.0079$ (Mann–Whitney). The arrows point to apoptotic nuclei. Scale bar = 100 μm. (**k**) Representative western blot analysis of caspase-2 (Casp2) processing at 24 h post-ischemia in the presence or absence of TRP601 or TRP901 injected (1 mg/kg, i.p.) at reperfusion. Ipsilateral penumbra zone (IL) and contralateral counterpart (CL) of hemispheres were dissected and homogenized before biochemical analysis. Co., control brains (without ischemia). (**l**) Detection of caspase-like activities at 24 h post-stroke in ipsilateral penumbra zones. Histograms show means of VDVADase, DEVDase, and LEHDase activities of animals i.p.-treated (■, $n = 5$) or not (□, $n = 5$) with TRP601 or TRP901. Note that kinetic analysis showed that the earliest and quantitatively major detected caspase-like activity is a VDVADase activity that reached 14 pmol/min/mg at $t = 5$ h post-ischemia, whereas neither DEVDase nor LEHDase activities were detected (Supplementary Figure S5). (**m**) TRP601 prevents cytochrome *c* release *in vivo*. A representative western blot analysis is shown. MF: mitochondrial fraction; CF: cytosolic fraction (CF). (**n**) Electron microscopy analysis of the mitochondria isolated from ischemic brains. The mitochondria isolated from vehicle-treated ipsilateral (IL), contralateral (CL) hemispheres, or TRP601-treated ipsilateral (IL + TRP601) hemispheres are shown. Each panel show an example of the dominant phenotype (> 60%) of the isolated mitochondria population

TRP601 is neuroprotective in neonatal excitotoxic brain injury. We next evaluated the effect of TRP601 after excitotoxic neonatal brain injury. In 5-day-old mice intracerebrally injected with ibotenate, a single administration of TRP601 (intraperitoneal (i.p.); 1 mg/kg) significantly reduced lesion volumes of cortical (40.96 ± 0.02%; $P<0.001$ Kruskal–Wallis *post hoc* Dunn's) ($V=0.23\pm0.07\,\mu m^3$, $n=16$ *versus* controls $V=0.37\pm0.06\,\mu m^3$, $n=16$) and white matter (48.87 ± 0.01% reduction; $P<0.01$) ($V=0.11\pm0.03\,\mu m^3$, $n=16$ *versus* controls $V=0.18\pm0.08\,\mu m^3$, $n=16$) regions (Figure 1g). In contrast, TRP901 (a DEVD-based preferential Casp3/Casp7 inhibitor) and TRP801 (a preferential Casp8 inhibitor[40]), both designed with the same chemistry as TRP601 (Supplementary Figure S2), did not confer brain protection against ibotenate challenge (Figure 1g). In these

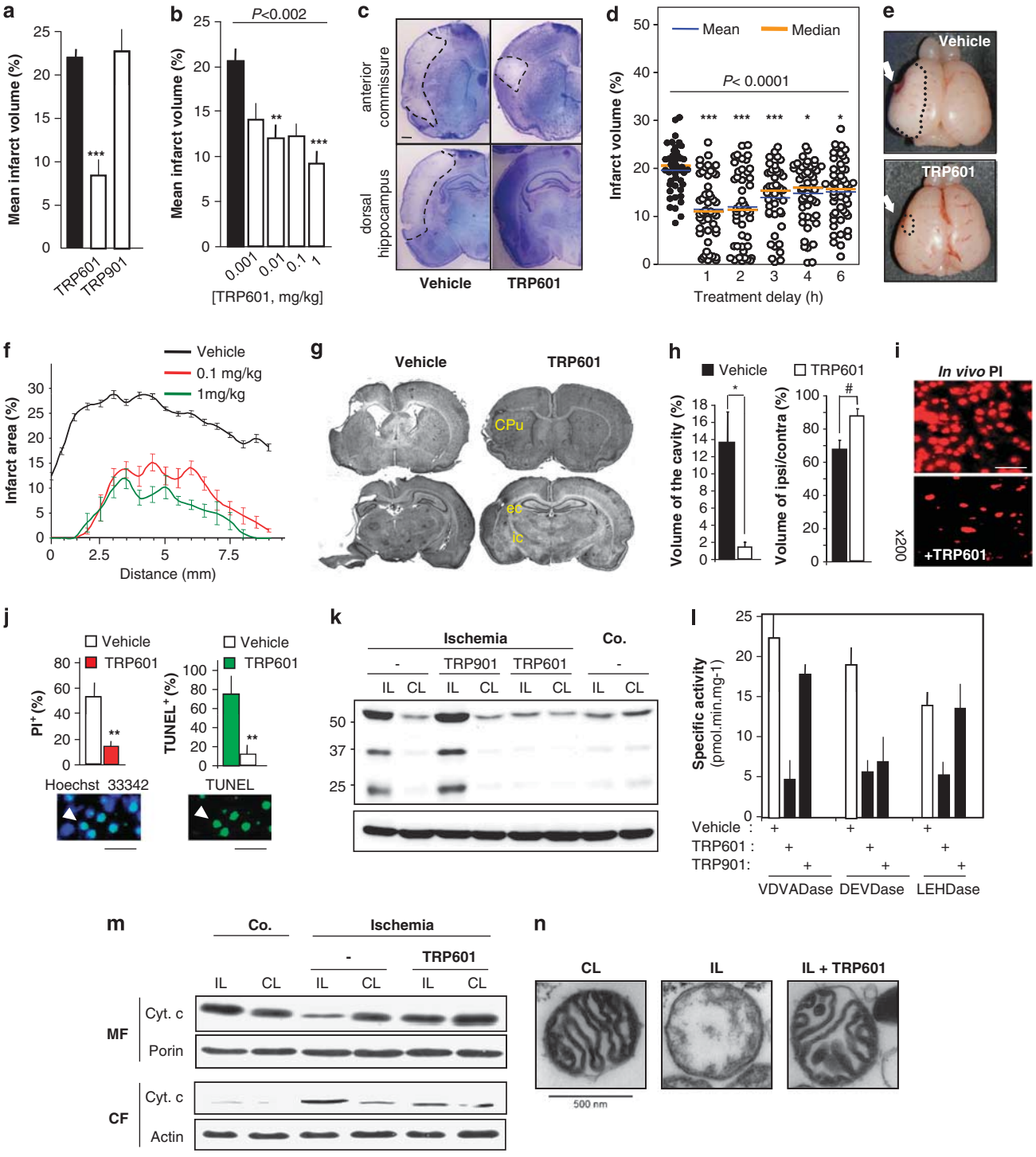

experimental conditions, TRP601 also reduced macrophage activation (43.51 ± 4.16% reduction; $P<0.0001$ Mann–Whitney) and astrogliosis (37.69 ± 3.15% reduction; $P<0.0001$ Mann–Whitney) as demonstrated by histological evaluation of lectine- (Figure 1h) and glial fibrillary acidic protein -positive (Figure 1i) cell densities, respectively. In addition, TRP601 strongly reduced the VDVADase-specific activity (73% reduction; $P=0.0079$ Mann–Whitney) when studied 8 h after ibotenate treatment (Figure 1j).

Having found recently that genetic inhibition of caspase-2 (Casp2) protects newborn mice from ischemic brain injury,[32] we further investigated the protective effect of TRP601 during Casp2 silencing. When TRP601 was administered in mice neonates treated with Casp2-specific siRNA, no significant additional protection was found against ibotenate, neither in the white matter nor in the cortical plate (Figure 1k and Supplementary Table S1). This suggests that, at least in this experimental setting, TRP601-mediated neuroprotection is Casp2 dependent.

TRP601 is neuroprotective in neonatal rats after ischemic stroke. We then investigated whether TRP601 might be operative in perinatal arterial stroke. The 7-day-old rat pups were subjected to a permanent occlusion of the MCAO and subsequent transient unilateral carotid ligation,[41] a model of neonatal ischemia with reperfusion that induces ipsilateral cortical injury associated with initiator and effector caspase processing,[42] extensive neuronal loss, inflammatory responses, nitric oxide production and the evolution of a cortical cavitary infarct.[41]

A single dose of TRP601 (5 mg/kg; i.p.) administered before occlusion induces a highly significant reduction (59%) of infarction (8.83 ± 1.8%; $n=24$) compared with the control (21.67 ± 1.65%; $n=15$) (Figure 2a). In contrast, the Casp3/Casp7 inhibitor TRP901 does not confer significant protection (22.2 ± 5.67%; $n=9$). TRP601 also produces significant reductions in cortical infarction when administered i.p. 1 h after the ischemic onset (i.e., at reperfusion) at doses between 1 μg/kg and 10 mg/kg ($n=103$; $P<0.002$ Kruskal–Wallis), with an optimal dose of 1 mg/kg (% infarction: 9.73 ± 1.9%; $n=18$, $P<0.001$ *post hoc* Dunn's; Figures 2b and c).

To determine the therapeutic time window of TRP601 in this perinatal stroke rat model, we designed a large protocol ($n=274$ rat pups, two independent experimenters) with randomized litters in each group ($P<0.0001$ Kruskal–Wallis; Figure 2d). When injected 2 h post-ischemia at 1 mg/kg (i.p.), TRP601-induced reduction of infarction was around 40% (% infarction: 11.78 ± 1.01%; $n=47$, $P<0.001$ *post hoc* Dunn's; Figure 2d) and remained significant (19.18% reduction) when TRP601 was added up to 6 h post-ischemia (% infarction: 16.01 ± 0.92%; $n=47$, $P<0.05$ *post hoc* Dunn's; Figure 2d).

The most clinically relevant administration route being i.v. injection, we set up similar experiments with post-ischemia intrajugular bolus of TRP601. Lesion scores on the entire brain and also section-based infarction quantifications converged to conclude that i.v. injected TRP601 (0.1–1 mg/kg; 1 h post-ischemia) considerably reduces ischemia-induced brain lesions along the rostro-caudal axis (Figures 2e and f), correlating with a significant neurological score amelioration in sensory and motor profiling assays (Table 2). We further investigated if cerebroprotection was long-lasting. At 21 days post-ischemia, the ipsilateral hemisphere of vehicle-treated animals exhibited a large cavity in the full thickness of the frontoparietal cortex (% cavitation: 12.5 ± 3.53%; $n=6$) and a tissue loss (32.33 ± 5.56%), which were markedly reduced in TRP601-treated rats (% cavitation: 1.42 ± 0.68%; $n=12$; % tissue loss: 12.1 ± 3.9%; Figures 2g and h), correlating with reduced astrogliosis (Supplementary Figure S3). Hence, in 7-day-old rats subjected to perinatal stroke, TRP601 provided sustained neuroprotection and neurological improvement, with a 6 h time window for administration.

TRP601 prevents apoptosis, caspase activation and cytochrome *c* release *in vivo*. Both *in vivo* propidium iodide staining and *ex vivo* terminal transferase dUTP nick-end labeling analysis of ipsilateral regions in brain sections from ischemic pups revealed a massive TRP601-sensitive cell death with apoptotic phenotype (Figures 2i and j). When administered at reperfusion, TRP601 prevents Casp2 processing (Figure 2k) and activation of all caspase-like activities, whereas TRP901 only reduces the DEVDase activity (Figures 2k and l). Previous reports had suggested that Casp2 may act directly and/or through Bid/Bax on mitochondrial membranes.[43,44] Using the mitochondria isolated from neonatal brain, we found that a mixture containing rCasp2 and full-length Bid induce TRP601-sensitive cytochrome *c* release, correlating with Casp2-induced Bid cleavage (Supplementary Figure S4). In addition, cytochrome *c* detection at 24 h post-ischemia in the ipsilateral cytosolic *versus* mitochondrial brain fraction indicates that TRP601 (added at reperfusion; i.p.) prevents the mitochondrial release of cytochrome *c in vivo* (Figure 2m), correlating with TRP601-mediated prevention of matrix swelling (Figure 2n).

TRP601 reduces HI brain injury. We next decided to determine whether the TRP601 pharmacological spectrum of use might include the most widely used neonatal HI model, where a focal brain injury occurs in 8-day-old rats after unilateral carotid ligation and exposure to 7.8 % oxygen for 50 min.[45] Indeed, a single dose of TRP601 (1 mg/kg; i.p.) administered just after hypoxia induces a significant reduction of infarct volume (30.3%; $P=0.0239$ Student's *t*-test; $V=60.22\pm8.47\,mm^3$, $n=24$ *versus* control $V=86.43\pm6.54\,mm^3$, $n=19$), percentage infarction (48.48 ± 3.13% *versus* 34.17 ± 4.69%; $P=0.0287$ Mann–Whitney; Figure 3a), and tissue loss (27.5%; $P=0.0412$ Mann–Whitney; $V=88.64\pm11.17\,mm^3$ *versus* control $V=122.29\pm6.84\,mm^3$; Figures 3b–d). An early TRP601-sensitive, but TRP901-insensitive, VDVADase activity (12 pmol/min per mg) was detected as early as 1 h post-HI in the cortex (Figure 3e). TRP601 also reduced various aspects of HI-induced white matter injury, including neurofilament degradation (NF68: 64.24 ± 8.5% *versus* controls 87.66 ± 5.32%; $P=0.049$ Mann–Whitney) (Figure 3f), oligodendroglial loss (CNPase: 69.56 ± 8.37% *versus* controls 91.29 ± 2.59%; $P=0.0307$ Student's *t*-test) (Figure 3g) and hypomyelination (MBP: 87.66 ± 8.8% *versus* controls 91.03 ± 2.6%; $P=0.041$ Student's *t*-test) (Figures 3h and i).

Table 2 Neurological benefit at 48 h: effect of TRP601 (i.v., 1 mg/kg, 1 h post-ischemia) on general behavioral profiles

	Naïve ($n=20$)	Isch.+vehicle ($n=20$)	Isch.+TRP601 ($n=20$)	*P*-values (χ^2) ($n=20$)
Spontaneous activity	1.8 ± 0.4	0.3 ± 0.6	1.1 ± 0.6	0.026×10^{-6}
Walking (circle *versus* straight)	0.3 ± 0.4	1.6 ± 0.6	0.8 ± 0.6	1.092×10^{-6}
Reaction to pain	1.7 ± 0.6	0.7 ± 0.6	1.2 ± 0.6	95.33×10^{-6}
Paw withdrawal	1.6 ± 0.6	0.3 ± 0.6	1.2 ± 0.6	0.261×10^{-6}
Mean lesion volume (mm^3)	0	24.3 ± 2.5	9.2 ± 2.3	NA

Sensorimotor neurological deficits were assessed in a blinded manner in 7-day-old rat pups. Animals were subjected to ischemia–reperfusion (as in Figures 2d–f) and treated with 1 mg/kg TRP601 (i.v., 1 h post-ischemia). At 48 h post-ischemia, pups were tested for the following neurological signs and reflexes: (i) spontaneous activity (spontaneous postural signs such as right forelimb flexion and thorax twisting and exploration of the cage); (ii) walking (after ischemia pups walk in circle rather than straight); (iii) reaction to pain (the pup escapes after the tail is pinched); (iv) paw withdrawal (pups withdraw paw from adhesive pad). Grading scale of neurological examination for each test item was: 2 for normal; 1 for intermediate; and 0 for abnormal. A neurological score (mean ± S.E.M.) was attributed for each test in each experimental condition (d.o.f. stands for degree of freedom in the χ^2 statistical test). NA, not applicable

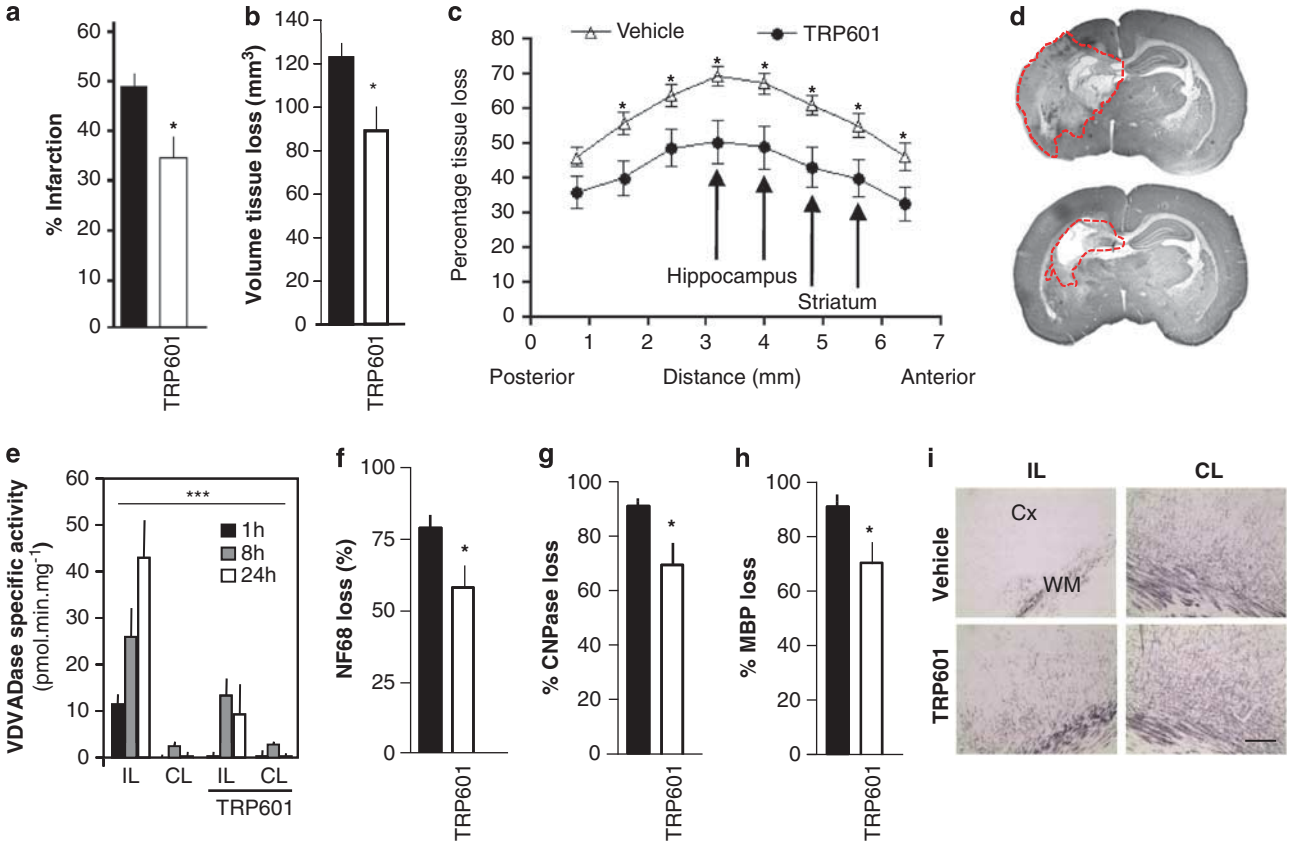

Figure 3 TRP601 reduces neonatal hypoxia–ischemia-mediated brain damage. The 8-day-old rats were subjected to transient unilateral carotid ligation and exposure to 7.8% oxygen during 50 min according to the Rice–Vannucci protocol. Pups were injected intraperitoneally (i.p.) with vehicle (■, $n=19$) or 1 mg/kg TRP601 (□, $n=24$) immediately after the end of hypoxia. Bars indicate S.E.M. $^*P<0.05$. (**a** and **b**) Histograms show % infarction (**a**) and mean volume tissue loss (**b**) measured at 72 h post-hypoxia–ischemia (HI) after microtubule-associated protein 2 (MAP2) staining at each anatomical level. (**c**) Rostro-caudal profiles. (**d**) Representative micrograph for MAP2-stained sections (bregma −3.14 mm). (**e**) Kinetics of Ac-VDVAD-AMC cleavage in the cortex from HI pups at 1, 8, or 24 h in the presence or absence of TRP601 (vehicle: $n=7$; TRP601: $n=8$ for each time point; $^{***}P<0.0001$ two-way analysis of variance (ANOVA)). (**f–i**) Immunohistochemistry of subcortical white matter in vehicle- (■, $n=19$) and 1 mg/kg TRP601- (□, $n=24$) treated pups. Histograms show: % NF68 loss (**f**), % CNPase loss (**g**), and % myelin basic protein (MBP) loss (**h**) measured at 72 h post-HI. (**i**) Representative micrograph for MBP staining in the subcortical white matter. Cx, cortex; WM, white matter. Scale bar = 200 μm

TRP601 does not modify physiological parameters. It is established that physiological variables can influence the outcomes of ischemic injury.[46] Importantly, when injected in rat pups, TRP601 (1 mg/kg) does not significantly alter physiological parameters, including systemic acid–base balance (arterial blood pH, partial tension of O_2, partial tension of CO_2 and plasma [HCO_3^-]), body weight, temperature, or heart rate (Table 3). Echography and transcranial color-coded duplex Doppler sonography showed that heart function and cerebral perfusion are unchanged in TRP601-exposed neonates (Table 3). In addition, telemetry experiments in vigil dogs indicated that

Table 3 Physiological variables in TRP601-treated rat pups

Parameters	Vehicle	TRP601
Blood hemodynamics and biochemistry		
Blood flow ($n=5$, ml/min)		
1 h	4.2 ± 0.9	3.6 ± 0.4
Resistance index[a] ($n=8$)		
1 h (cerebral artery)	0.68 ± 0.01	0.64 ± 0.03
Bleeding time ($n=10$)		
1 h	319 ± 34	395 ± 103
Arterial pH ($n=8$)		
1h	7.42 ± 0.03	7.42 ± 0.02
PaO_2 ($n=8$, mm Hg)		
1 h	70.84 ± 6.38	69.82 ± 2.24
$PaCO_2$ ($n=8$, mm Hg)		
1 h	37.96 ± 2.64	42.06 ± 2.58
HCO_3^- ($n=8$, mM)		
1 h	24.16 ± 0.61	26.30 ± 0.76
Cardiac physiology		
Heart rate ($n=8$, beat/min)		
1 h	345 ± 13	344 ± 12
LVEDd ($n=8$, mm)		
1 h	0.293 ± 0.015	0.310 ± 0.015
LVO ($n=8$, ml/min)		
1 h	0.135 ± 0.009	0.157 ± 0.015
Fractional shortening ($n=8$, %)		
1h	54.39 ± 0.96	49.97 ± 2.11
VTIm ($n=8$)		
1 h	4.05 ± 0.11	3.92 ± 0.29
Core temperature ($n=10$, °C)		
1 h	36.60 ± 0.28	36.40 ± 0.67
3 h	36.39 ± 0.54	36.40 ± 0.67
48 h	36.63 ± 0.23	36.80 ± 0.23
Body weight ($n=10$, g)		
Co.	19.49 ± 1.43	19.18 ± 0.95
1 h	19.35 ± 1.72	20.40 ± 1.67
48 h	20.96 ± 1.25	20.90 ± 0.67
14 days	69.56 ± 1.60	62.00 ± 2.50

Blood hemodynamics, biochemistry, cardiac physiology, temperature, and body weight were evaluated before and 1 h after TRP601 (1 mg/kg) or vehicle injection. Anterior cerebral arteries were located by transcranial color-coded duplex sonography to measure peak systolic (V_s) and maximum end-diastolic (V_d) velocities. Resistive index (RI) was calculated as follows: $RI = ((V_s - V_d)/V_s)$, and corresponds to an index of cerebral perfusion. For cardiac physiology, the left ventricle (LV) was imaged in short axis view, and diastolic diameter (LVEDd) was defined as the largest LV area. The fractional shortening was calculated with the following formula: $FS\ (\%) = ((LVEDd - LVEDs)/LVEDd) \times 100$. LVED corresponds to left ventricular end-systolic diameter. A pulsed-wave Doppler spectrum of aortic outflow was recorded from supra-sternal view to evaluate left ventricular output (LVO). Velocity–time integral (VTI) of aortic flow, aortic root diameter (CSA), and heart rate (HR) were measured to calculate LVO as follows: $LVO = CSA \times VTI \times HR$. A pulsed-wave Doppler spectrum of mitral inflow (VTIm) was recorded from the apical four-chamber view as an index of diastolic function. Statistical analysis was performed by a mean comparison using a Scheffe test. [a]Transcranial Doppler sonography

vital signs, heart rate, and electrocardiogram profile including QT interval corrected for heart rate were not affected by TRP601 up to the maximal dose tested (i.e., 3 mg/kg, i.v.), suggesting low potential for fatal tachyarrhythmia. Supra-pharmacological doses of TRP601 in rats had no impact on central nervous system functions, including behavior, spatial activity, coordination, and memory.

To exclude the potential risk that TRP601 might affect the physiological programmed cell death, which contributes to normal brain maturation, TUNEL (terminal deoxynucleotidyl transferase dUTP nick-end labeling) *ex vivo* studies were performed, and it was found that rat pups treated with TRP601 at postnatal days 5 and 7 (after birth) showed no significant changes in developmental cell death in the brain (Supplementary Table S2). In addition, histological analysis in 7-day-old rat pups treated with high doses of TRP601 found no influence on forebrain, middle brain, and hindbrain maturation at 21 days of age (data not shown).

TRP601 safety profile in adult and neonates support further translational steps. The bench to bedside translation of any drug dedicated to the neonatal population requires specific PK/PD considerations together with combined toxicology evaluation in both adult and neonates. For these reasons, having verified that TRP601 has no hemolytic potency, no effect on bleeding time, no impact on platelet aggregation, and low toxicities on various cultured primary cells, we then investigated toxicology in adult animals, together with dedicated studies in rodent and non-rodent neonates (see Supplementary Materials and Methods). In multiple-dose regulatory studies in adult dogs, no TRP601-related cytotoxic effects were observed following i.v. administration for 14 days at doses up to 3 mg/kg per day. A good vascular and perivascular local tolerance was found in rabbit ear. TRP601 was found not to be genotoxic when evaluated in a battery of *in vitro* and *in vivo* assays, and showed no antigenic response in rat. In 7-day-old rat pups, single-dose administrations of TRP601 indicated low toxicity of TRP601 (DL_{50}i.v. = 60 mg/kg; DL_{30}i.p. > 200 mg/kg). Studies with multiple-dose i.v. injections (once every 3 days during a 2-week period, starting on postnatal day 1 in newborn *Beagle* dogs) showed no adverse effect level at 15 mg/kg per injection once every 3 days.

Discussion

Neonatal ischemic brain injury triggers multiple pathways of oxidant stress, inflammation, and excitotoxicity that lead to massive cellular death in the ischemic territory. Caspase-dependent programmed cell death importantly contributes to this fate.[7,9,10,14,15,23,24,32,42] In contrast to previous generations of aspartyl-fluoromethylketone (D-fmk)-based inhibitors (e.g., z-VAD-fmk (*N*-benzyloxycarbonyl-Val-Ala-Asp(Ome)-fluoromethylketone), boc-D-fmk (Boc-Asp (OMe)-fluoromethylketone)), aspartyl-methyloxyphenylketone-based inhibitors (e.g., Q-VD-OPh) only target the caspase family, efficiently inhibit (all) caspases, have low *in vivo* toxicity, and present enhanced pharmacological properties.[10,16,25,33] Our results show that pharmacological inhibition of a subfamily of caspases (Casp2, Casp3) with the pentapeptide-mOPh derivative, TRP601, reduces cortical and white matter damage in the neonatal brain after excitotoxicity, arterial stroke, and HI. In all of these experimental paradigms, TRP601 also reduces gliosis, an inflammatory response to brain ischemia. It has been demonstrated recently that caspase-8 and Casp3/7 are involved in regulating microglia activation.[47] Consequently, beside its direct protective effect on neurons (as observed in primary cortical cell cultures), it might be important to investigate whether TRP601 (or the active metabolite Δ2Me-TRP601) could also exert cerebro-protective effects through targeting the microglia.

Our results indicate that TRP601 and its active metabolite(s) (e.g., Δ2Me-TRP601) inhibit Casp3 and Casp2 *in vitro* and *in vivo*. We also provide evidences suggesting that TRP601 interrupts the mitochondrial (intrinsic) pathway of apoptosis in the immature brain, possibly at the level of Casp-2-mediated Bid cleavage, and upstream cytochrome *c* release.[39] We have recently reported that Casp2$^{-/-}$ mice subjected to neonatal HI presented significantly lower cerebral infarction, reduced white matter injury, and reduced Casp3 activation in the thalamus and hippocampus.[32] Lesion sizes and Casp3 activation were also found reduced in Casp2-deficient newborn mice subjected to excitotoxicity.[32] In addition, we show here that combined administration of TRP601 with Casp2 silencing did not show any additive effect against ibotenate challenge. This suggests that the TRP601-mediated neuroprotection is at least, in part, Casp2-dependent. Taken together, our data suggest that the *in vivo* observed neuroprotection and Casp3 inhibition by TRP601 are at least, in part, Casp2-dependent. However, we could not formally exclude that part of the neuroprotective effect of TRP601 could be related to a direct Casp3 inactivation by TRP601 or Δ2Me-TRP601 (this latter being a very powerful Casp3 inhibitor *in vitro*). As the selective Casp3 inhibitor M826 was previously found neuroprotective against neonatal HI,[24] one can suggest that the use of a group-II caspase inhibitor might be of therapeutic interest to cover different conditions, developmental stages, or regional mechanisms, where Casp3/7 and Casp2 are variably expressed and activated through different pathways.

Irrespective of these mechanistic considerations, TRP601 is a lead candidate for neuroprotective strategy in a variety of perinatal brain injury conditions. The lack of detectable side effects following *in vivo* administration of TRP601 to newborn rodents and dogs support its further evaluation, possibly in combination with hypothermia[5] or other candidate treatments.[6,48]

Materials and Methods

Animal models. Three different animal models were used: neonatal stroke, excitotoxicity, and HI. Neonatal stroke (focal brain ischemia with reperfusion in the 7-day-old rat) was carried out according to Renolleau *et al.*[10,41] For HI, 8-day-old rats or alternatively 9-day-old mice were subjected to unilateral ligation of the left carotid artery, followed by hypoxia (7.8% O_2 for rats and 10% O_2 for mice, 36°C) for 50 min, as described.[32] For drug-induced excitotoxicity, ibotenate was administered i.c.v. to 5-day-old mice, as described.[32] Details for each animal models are given in Supplementary Material and Methods. SiRNAs were prepared as a solution in JetSI according to the manufacturer's recommendations (PolyPlus-transfection, Illkirch, France). Final solution contained RNAse free water, 0.08 mM DOPE, 0.24% chloroform/7% EtOH, glucose 12.5%, and 0.04 mM JetSI. For intracerebral siRNA administration, 0.4 μg siRNA/mice were administered (volume of injection = 2 μl) 24 h before ibotenate. SiRNA sequences and primers for PCR were reported previously.[32]

Primary cortical neuron culture and cell death analysis. Primary cortical neurons from E14 Swiss mice embryos (Janvier, Le Genest-St-Isle, France) were cultured in N5 complete medium up to 6 DIV and subjected to serum deprivation in the absence or presence of TRP601, or alternatively were transfected with siRNAs using Lipofectamine 2000 (Invitrogen, Carlsbad, CA, USA) 24 h before serum withdrawal. To monitor cell death parameters, neurons were co-stained with Hoechst 33342 (nuclear condensation; Sigma, Saint Louis, MO, USA), JC-1 (5,5′,6,6′-tetrachloro-1,1′, 3,3′-tetraethyl-benzimidazolylcarbocyanine iodide) (mitochondrial transmembrane potential-sensitive probe), and 7-amino actinomycin D (plasma membrane permeabilization; Sigma), and then subjected to fluorescence microscopy (DM IRB; Leica, Rueil-Malmaison, France) and flow cytometry (FACSCalibur; Becton Dickinson, San Jose, CA, USA) analysis, as described previously.[39] *In cellula* caspase activities were detected using FAM-conjugated peptides (CaspaTag fluorescein Caspase Activity Kits; Q-Biogen, MP Biomedicals, Illkirch, France), as described.[39]

Preparation and use of drug solutions. Synthesis of TRP601/ORPHA133563 (also known as OPH016) is described in Supplementary Materials and Methods). Research batches where synthesized in-house (Dr. Richard Casimir). Additional batches were custom synthesized by MP Biomedicals or alternatively by NeoMPs (PolyPeptide group, Strasbourg, France). For regulatory safety studies, TRP601 process development and manufacturing of GMP batches were subcontracted to NeoMPs (PolyPeptide group). For *in vitro* studies TRP601 ($C_{40}H_{48}F_2N_6O_{11}$; MW: 826.84), Δ2Me-TRP601 ($C_{38}H_{44}F_2N_6O_{11}$; MW: 798.79), TRP801 (MW: 771.76), and TRP901 (MW: 799.77) were initially solubilized in 100% DMSO. The final concentration of DMSO was $\leq$1%. For *in vivo* efficacy experiments, TRP601, TRP801, and TRP901 were formulated in 0.9% NaCl containing 10% DMSO for i.p. administration or 2.4% Tween 20 for i.v. administration. I.v. administration of TRP601 to 7-day-old rats was carried out intrajugularly using 27-gauge needles. All stock solutions and formulations were verified using RP-HPLC. TRP601 has a high degree of lipophilicity (partition coefficient, Log $P_{octanol/water} = 3.89$) and exhibits one pK_a of 1.1 (assigned to the quinoleine group), strongly suggesting that it remains neutral in the plasma. Bioanalysis of TRP601 in fluids and organ homogenates was conducted by LC/MS/MS analysis with a precision of 1.00 ng/ml in the plasma and 3.00 ng/g in exsanguined brain homogenates (ADME Bioanalyses, Vergeze, France).

Molecular modeling. Starting from the crystal structure of the caspase-2-inhibitor (Ac–LDESD–CHO) complex (1PYO), pentapeptide inhibitors (including Ac–VDVAD–CHO and TRP601) were studied in an uncharged form and at a dielectric constant of 1, using either Insight II or Discovery Studio 2.0 softwares (Accelrys, San Diego, CA, USA). See details in Supplementary Materials and Methods.

***In vitro* enzymatic assays.** Kinetics were performed according to the continuous method. Assays of chromogenic substrate cleavage contained in 100 μl caspase buffer (20 mM HEPES, pH 7.4, 0.1% CHAPS, 5 mM DTT, 2 mM EDTA), 117 ng of human active recombinant caspase-2 (Biomol, Plymouth, PA, USA) or 20 ng of human active recombinant caspase-3 (Sigma; no. C5974), and 100 μM of chromogenic substrate (Ac–DEVD–*para*-nitroaniline (*p*NA) for Casp3 and Ac–VDVAD–*p*NA for Casp2) in the presence of a range of concentrations of inhibitors. For Casp2 assays, the buffer was supplemented with 1 M succinate (kosmotrope agent). Cleavage of the chromogenic substrate as a function of time was monitored at 405 nm, and the initial velocity (V_0) was determined from the linear portion of the progress curve. The formation of *p*NA was followed every 30 s for 150 min at 37°C with a microtiter plate reader (Paradigm Multi-Mode Microplate Detection Platform, SoftMax Pro 5.2 software; Molecular Devices, St. Grégoire Cédex, France). V_0, relative velocities, K_m, and IC_{50} were determined from experimental data using the GraphPad Prism 5.01 software program. Standard deviations of the reported values were below 10%. Inhibitor binding affinity (dissociation constant, K_i) and first-order rate constant (k_3) parameters were estimated using *R* (http://www.R-project.org) to fit the following equation from Wu and Fritz[49]:

$$[P]_t = [E]_0 \left(\frac{[S]K_i}{[I]K_s}\right)\left(\frac{k_s}{k_3}\right)\left[1 - e^{-k_3 t/(1+(K_i/[I])(1+[S]/K_s))}\right]$$

Other *in vitro* assays for calpains, cathepsins, and granzyme activities were performed as described.[33]

***Ex vivo* biochemistry.** Brains of rat or mice pups were removed just after decapitation. Contralateral and ipsilateral hemispheres were frozen immediately and kept at −80°C. Alternatively, the ipsilateral hemisphere was rapidly micro-dissected (at 4°C) to mainly select the lesioned area (i.e., the estimated penumbra zone for the neonatal stroke model). Brain samples processing and related biochemical analyses are described in Supplementary Material and Methods.

Physiological parameters. Blood gas analyses and hemodynamic evaluations conducted in newborn rats are described in Supplementary Materials and Methods.

Safety pharmacology and toxicology. Safety experiments conducted in newborn dogs and rats are described in Supplementary Materials and Methods.

Statistics. Statistical analyses were conducted with Prism 4.0. Data are presented as mean ± S.E.M. and were first analyzed with a KS normality test. When the data passed the normality test, the appropriate parametric test has been applied (Student's *t*-test or ANOVA), followed by the suitable *post hoc* test if necessary (Bonferroni test). When the data did not pass the normality test, the appropriate non-parametric test has been applied (Mann–Whitney or Kruskal–Wallis tests), followed by the suitable *post hoc* test if necessary (Dunn's test). Neurological scores were statistically analyzed with a χ^2. Statistical significance is indicated by a single asterisk ($P<0.05$), and two or three asterisks ($P<0.01$ or <0.001, respectively).

Conflict of Interest

Some of the authors (DC, SA, MB, RC, MS, A-PT, EB, and EJ) were former employees of a biopharmaceutical company (Theraptosis SA, Paris, France) that closed down in late 2008. Other authors (SR, SH, LS, CR, JH, GD, YC, XW, MH, J-MR, SM, AL, PR, JM, HH, PG, CC-M) declare no conflict of interest. First public disclosure of TRP601-related data occurred in June 2008 (6th Hershey Conference, Ecquevilly, France). TRP601 rights were acquired in 2009 by Chiesi Pharmaceutici SpA, Parma, Italy (http://www.chiesigroup.com/web/guest/chi-siamo/key-figures/report-finanziari; Annual Report 2009, p 50).

Acknowledgements. We thank Professor A David Edwards, Professor Carol Troy, Professor Marie-Lise Gougeon, Professor Michèle Reboud-Ravaux, Dr. Gilles Guichard, and Tinoray Jacotot for discussion and advice. We also thank Alain Langonné, Christelle Garraud-Moquereau, and Anna-Lena Leverin for technical assistance, and Dr. Isabelle Margail (University Paris V, Paris, France) for MCAO in adult mice; Dr. Christelle Gélis and Dr. Patrick Duchêne (ADME Bioanalyse, Vergèze, France) for bioanalysis; Dr. Jean-Michel Caillaud (Biodoxis SA, Romainville, France) and Dr. Palate (CIT, Evreux, France) for histopathology examinations; Dr. Olivier Foulon, Dr. Rhian Davies, Dr. Pierre-Olivier Guillaumat, and Dr. Valerie Haag (CIT) for animal toxicology contributions and expertise; and Dr. Françoise Brunner for excellent advice during drug development. This work was supported by grants from the French Ministry of Research (No. 01H0476 to EJ; No. 01H0477 to JM), Inserm, Foundation *Grace de Monaco* (to CC-M and PG), *Agence Nationale pour la Valorisation de la Recherche* (ANVAR; No. R0209330Q to EJ), *Medical Research Council* strategic award (MRC, UK, P19381 to HH), University Paris 7, Premup, Medical Research Council (VR, Sweden, 2006-3396 to HH), ALF-LUA (Sweden, ALFGBG2863 to HH), and the Sixth Framework Programme of the European Commission (STREP – *Neobrain* consortium, Contract No. LSHM-CT-2006-036534 to HH, PG, and EJ).

1. Lawn JE, Lee AC, Kinney M, Sibley L, Carlo WA, Paul VK *et al.* Two million intrapartum-related stillbirths and neonatal deaths: where, why, and what can be done? *Int J Gynaecol Obstet* 2009; **107**: S5.
2. du Plessis AJ, Volpe JJ. Perinatal brain injury in the preterm and term newborn. *Curr Opin Neurol* 2002; **15**: 151–157.
3. Ferriero DM. Neonatal brain injury. *N Engl J Med* 2004; **351**: 1985–1995.
4. Lawn JE, Bahl R, Bergstrom S, Bhutta ZA, Darmstadt GL, Ellis M *et al.* Setting research priorities to reduce almost one million deaths from birth asphyxia by 2015. *PLoS Med* 2011; **8**: e1000389.
5. Azzopardi DV, Strohm B, Edwards AD, Dyet L, Halliday HL, Juszczak E *et al.* Moderate hypothermia to treat perinatal asphyxial encephalopathy. *N Engl J Med* 2009; **361**: 1349–1358.
6. Gonzalez FF, Ferriero DM. Neuroprotection in the newborn infant. *Clin Perinatol* 2009; **36**: 859–880.
7. Northington FJ, Zelaya ME, O'Riordan DP, Blomgren K, Flock DL, Hagberg H *et al.* Failure to complete apoptosis following neonatal hypoxia-ischemia manifests as 'continuum' phenotype of cell death and occurs with multiple manifestations of mitochondrial dysfunction in rodent forebrain. *Neuroscience* 2007; **149**: 822–833.
8. Kaindl AM, Favrais G, Gressens P. Molecular mechanisms involved in injury to the preterm brain. *J Child Neurol* 2009; **24**: 1112–1118.
9. Gill R, Soriano M, Blomgren K, Hagberg H, Wybrecht R, Miss MT *et al.* Role of caspase-3 activation in cerebral ischemia-induced neurodegeneration in adult and neonatal brain. *J Cereb Blood Flow Metab* 2002; **22**: 420–430.
10. Renolleau S, Fau S, Goyenvalle C, Joly LM, Chauvier D, Jacotot E *et al.* Specific caspase inhibitor Q-VD-OPh prevents neonatal stroke in P7 rat: a role for gender. *J Neurochem* 2007; **100**: 1062–1071.
11. Wang X, Carlsson Y, Basso E, Zhu C, Rousset CI, Rasola A *et al.* Developmental shift of cyclophilin D contribution to hypoxic–ischemic brain injury. *J Neurosci* 2009; **29**: 2588–2596.
12. Edwards AD, Yue X, Cox P, Hope PL, Azzopardi DV, Squier MV *et al.* Apoptosis in the brains of infants suffering intrauterine cerebral injury. *Pediatr Res* 1997; **42**: 684–689.
13. Hagberg H, Mallard C, Rousset CI, Wang X. Apoptotic mechanisms in the immature brain: involvement of mitochondria. *J Child Neurol* 2009; **24**: 1141–1146.
14. Zhu C, Wang X, Xu F, Bahr BA, Shibata M, Uchiyama Y *et al.* The influence of age on apoptotic and other mechanisms of cell death after cerebral hypoxia–ischemia. *Cell Death Differ* 2005; **12**: 162–176.
15. Wang X, Han W, Du X, Zhu C, Carlsson Y, Mallard C *et al.* Neuroprotective effect of Bax-inhibiting peptide on neonatal brain injury. *Stroke* 2010; **41**: 2050–2055.
16. Zhu C, Wang X, Huang Z, Qiu L, Xu F, Vahsen N *et al.* Apoptosis-inducing factor is a major contributor to neuronal loss induced by neonatal cerebral hypoxia–ischemia. *Cell Death Differ* 2007; **14**: 775–784.
17. Thornberry NA, Lazebnik Y. Caspases: enemies within. *Science* 1998; **281**: 1312–1316.
18. Talanian RV, Brady KD, Cryns VL. Caspases as targets for anti-inflammatory and anti-apoptotic drug discovery. *J Med Chem* 2000; **43**: 3351–3371.
19. Yuan J, Yankner BA. Apoptosis in the nervous system. *Nature* 2000; **407**: 802–809.
20. Talanian RV, Quinlan C, Trautz S, Hackett MC, Mankovich JA, Banach D *et al.* Substrate specificities of caspase family proteases. *J Biol Chem* 1997; **272**: 9677–9682.
21. Garcia-Calvo M, Peterson EP, Leiting B, Ruel R, Nicholson DW, Thornberry NA *et al.* Inhibition of human caspases by peptide-based and macromolecular inhibitors. *J Biol Chem* 1998; **273**: 32608–32613.
22. Garcia-Calvo M, Peterson EP, Rasper DM, Vaillancourt JP, Zamboni R, Nicholson DW *et al.* Purification and catalytic properties of human caspase family members. *Cell Death Differ* 1999; **6**: 362–369.
23. Cheng Y, Deshmukh M, D'Costa A, Demaro JA, Gidday JM, Shah A *et al.* Caspase inhibitor affords neuroprotection with delayed administration in a rat model of neonatal hypoxic–ischemic brain injury. *J Clin Invest* 1998; **101**: 1992–1999.
24. Han BH, Xu D, Choi J, Han Y, Xanthoudakis S, Roy S *et al.* Selective, reversible caspase-3 inhibitor is neuroprotective and reveals distinct pathways of cell death after neonatal hypoxic–ischemic brain injury. *J Biol Chem* 2002; **277**: 30128–30136.
25. Joly LM, Mucignat V, Mariani J, Plotkine M, Charriaut-Marlangue C. Caspase inhibition after neonatal ischemia in the rat brain. *J Cereb Blood Flow Metab* 2004; **24**: 124–131.
26. Puyal J, Vaslin A, Mottier V, Clarke PG. Postischemic treatment of neonatal cerebral ischemia should target autophagy. *Ann Neurol* 2009; **66**: 378–389.
27. Karatas H, Aktas Y, Gursoy-Ozdemir Y, Bodur E, Yemisci M, Caban S *et al.* A nanomedicine transports a peptide caspase-3 inhibitor across the blood–brain barrier and provide1neuroprotection. *J Neurosci* 2009; **29**: 13761–13769.
28. Kuida K, Zheng TS, Na S, Kuan C, Yang D, Karasuyama H *et al.* Decreased apoptosis in the brain and premature lethality in CPP32-deficient mice. *Nature* 1996; **384**: 368–372.
29. Kuida K, Haydar TF, Kuan CY, Gu Y, Taya C, Karasuyama H *et al.* Reduced apoptosis and cytochrome *c*-mediated caspase activation in mice lacking caspase 9. *Cell* 1998; **94**: 325–337.
30. Bergeron L, Perez GI, Macdonald G, Shi L, Sun Y, Jurisicova A *et al.* Defects in regulation of apoptosis in caspase-2-deficient mice. *Genes Dev* 1998; **12**: 1304–1314.
31. West T, Atzeva M, Holtzman DM. Caspase-3 deficiency during development increases vulnerability to hypoxic–ischemic injury through caspase-3-independent pathways. *Neurobiol Dis* 2006; **22**: 523–537.
32. Carlsson Y, Schwendimann L, Vontell R, Rousset CI, Wang X, Lebon S *et al.* Genetic inhibition of caspase-2 reduces hypoxic–ischemic and excitotoxic neonatal brain injury. *Ann Neurol* 2011; e-pub ahead of print 28 March 2011; doi:10.1002/ana.22431.
33. Chauvier D, Ankri S, Charriaut-Marlangue C, Casimir R, Jacotot E. Broad-spectrum caspase inhibitors: from myth to reality? *Cell Death Differ* 2007; **14**: 387–391.
34. Zhu C, Qiu L, Wang X, Hallin U, Candé C, Kroemer G *et al.* Involvement of apoptosis-inducing factor in neuronal death after hypoxia–ischemia in the neonatal rat brain. *J Neurochem* 2003; **86**: 306–317.
35. Linton SD, Aja T, Armstrong RA, Bai X, Chen LS, Chen N *et al.* First-in-class pan caspase inhibitor developed for the treatment of liver disease. *J Med Chem* 2005; **48**: 6779–6782.
36. Leung-Toung R, Zhao Y, Li W, Tam TF, Karimian K, Spino M *et al.* Thiol proteases: inhibitors and potential therapeutic targets. *Curr Med Chem* 2006; **13**: 547–581.
37. McStay GP, Salvesen GS, Green DR. Overlapping cleavage motif selectivity of caspases: implications for analysis of apoptotic pathways. *Cell Death Differ* 2008; **15**: 322–331.
38. Schweizer A, Briand C, Grutter MG. Crystal structure of caspase-2, apical initiator of the intrinsic apoptotic pathway. *J Biol Chem* 2003; **278**: 42441–42447.
39. Chauvier D, Lecoeur H, Langonné A, Borgne-Sanchez A, Mariani J, Martinou JC *et al.* Upstream control of apoptosis by caspase-2 in serum-deprived primary neurons. *Apoptosis* 2005; **10**: 1243–1259.
40. Dzietko M, Boos V, Sifringer M, Polley O, Gerstner B, Genz K *et al.* A critical role for Fas/CD-95 dependent signaling pathways in the pathogenesis of hyperoxia-induced brain injury. *Ann Neurol* 2008; **64**: 664–673.
41. Renolleau S, Aggoun-Zouaoui D, Ben-Ari Y, Charriaut-Marlangue C. A model of transient unilateral focal ischemia with reperfusion in the P7 neonatal rat: morphological changes indicative of apoptosis. *Stroke* 1998; **29**: 1454–1461.
42. Villapol S, Bonnin P, Fau S, Baud O, Renolleau S, Charriault-Marlangue C. Unilateral blood flow decrease induces bilateral and symmetric responses in the immature brain. *Am J Pathol* 2009; **175**: 2111–2120.

43. Guo Y, Srinivasula SM, Druilhe A, Fernandes-Alnemri T, Alnemri ES. Caspase-2 induces apoptosis by releasing proapoptotic proteins from mitochondria. *J Biol Chem* 2002; **277**: 13430–13437.
44. Robertson JD, Enoksson M, Suomela M, Zhivotovsky B, Orrenius S. Caspase-2 acts upstream of mitochondria to promote cytochrome c release during etoposide-induced apoptosis. *J Biol Chem* 2002; **277**: 29803–29809.
45. Andiné P, Thordstein M, Kjellmer I, Nordborg C, Thiringer K, Wennberg E *et al.* Evaluation of brain damage in a rat model of neonatal hypoxic–ischemia. *J Neurosci Methods* 1990; **35**: 253–260.
46. Hunter AJ, Green AR, Cross AJ. Animal models of acute ischaemic stroke: can they predict clinically successful neuroprotective drugs? *Trends Pharmacol Sci* 1995; **16**: 123–128.
47. Burguillos MA, Deierborg T, Kavanagh E, Persson A, Hajji N, Garcia-Quintanilla A *et al.* Caspase signalling controls microglia activation and neurotoxicity. *Nature* 2011; **472**: 319–324.
48. Gonzalez FF, Ferriero DM. Therapeutics for neonatal brain injury. *Pharmacol Ther* 2008; **120**: 43–53.
49. Wu JC, Fritz LC. Irreversible caspase inhibitors: tools for studying apoptosis. *Methods* 1999; **17**: 320–328.

Supplementary Information accompanies the paper on Cell Death and Disease website (http://www.nature.com/cddis)